Contribution from the Department of Chemistry, The University of Michigan, Ann Arbor, Michigan 48109, and the Molecular Structure Center, Indiana University, Bloomington, Indiana 47405

Metal-Metal-Bonded Complexes of the Early Transition Metals. 8. Tertiary Alkylphosphine Adducts of $W_2(O_2CCF_3)_4$ ($W \equiv W$)[1]

D. J. SANTURE,[2a] J. C. HUFFMAN,[2b] and A. P. SATTELBERGER*[2a]

Received June 28, 1983

$W_2(O_2CCF_3)_4$ reacts with 2 equiv of PR_3 (R = Me, Et, *n*-Bu) in toluene to give adducts of stoichiometry $W_2(O_2CCF_3)_4 \cdot 2PR_3$. These complexes have been characterized by infrared, ^{19}F NMR, and $^{31}P\{^1H\}$ NMR spectroscopies. A single isomer, with equatorially bound phosphines, is observed in solution (−50 to +25 °C) in each case. X-ray structural studies on the P-*n*-Bu_3 derivative show that this isomer has a C_{2h} core. $W_2(O_2CCF_3)_4 \cdot 2PMe_3$ reacts with excess PMe_3 in toluene to provide the isolable trisadduct $W_2(O_2CCF_3)_4 \cdot 3PMe_3$. The structure of this complex was deduced from ^{19}F and $^{31}P\{^1H\}$ NMR experiments and confirmed by X-ray crystallography. $W_2(O_2CCF_3)_4 \cdot 3PMe_3$ has three equatorially bound phosphines, two of which are in a cis configuration on one of the metal centers. Crystal data (at −160 °C) are as follows: for $W_2(O_2CCF_3)_4 \cdot 2P(C_4H_9)_3$, monoclinic space group $I2/a$, a = 19.240 (6) Å, b = 10.379 (2) Å, c = 21.522 (6) Å, β = 93.39 (2)°, V = 1224.40 Å^3, Z = 4, d_{calcd} = 1.896 g cm^{-3}; for $W_2(O_2CCF_3)_4 \cdot 3P(CH_3)_3$, orthorhombic space group $Pc2_1n$, a = 9.870 (3) Å, b = 15.002 (6) Å, c = 21.118 (10) Å, V = 3126.87 Å^3, Z = 4, d_{calcd} = 2.226 g cm^{-3}.

Introduction

The tungsten(II) carboxylates, $W_2(O_2CR)_4$, are recent additions[3] to the growing family of quadruply metal-metal-bonded tungsten compounds,[4] and their chemistry is being developed in this laboratory[5] and elsewhere.[6] One of the questions we want to address in our investigations is the following: To what extent are the chemistries of $Mo_2(O_2CR)_4$ and $W_2(O_2CR)_4$ complexes and their derivatives similar or dissimilar? Previously we have shown[3,5] that tetrakis(trifluoroacetato)ditungsten, $W_2(TFA)_4$ (**1**), like its molybdenum homologue,[7] forms an axial or class I adduct (A) with triphenylphosphine. The phosphine ligands in these $M_2(TFA)_4 \cdot 2PPh_3$ complexes are weakly bound in the solid state (Mo-P = 3.07 (5) Å;[8] W-P = 2.97 [2] Å[5]), and both adducts are extensively dissociated in solution (eq 1).[5,7]

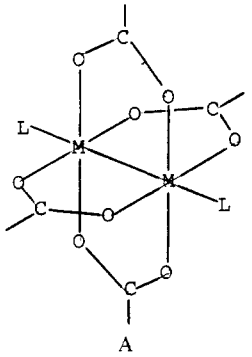

A

$$M_2(TFA)_4 \cdot 2PPh_3 \rightleftharpoons M_2(TFA)_4 + 2PPh_3 \quad (1)$$

With small basic tertiary phosphines, e.g., triethylphosphine, $Mo_2(TFA)_4$ forms equatorial or class II adducts;[7] one isomer of this class is shown by structure B. We have examined the reactions of **1** with several of these phosphines, and our results, including the structural characterization of two new adducts of **1**, are reported herein.

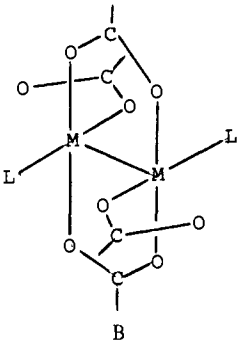

B

Results and Discussion

Synthesis and Physicochemical Properties of $W_2(TFA)_4 \cdot 2PR_3$ Compounds. Toluene solutions of **1** react rapidly with PMe_3, PEt_3, or P-*n*-Bu_3 to yield red to red-orange complexes, **2a-c**, according to eq 2. The use of excess alkylphosphine must be avoided only in the case of trimethylphosphine as this leads to the formation of a stable tris(trimethylphosphine) adduct, which is described below. All of these complexes are air sensitive in the solid state and especially in solution. Adducts **2b** and **2c** are soluble in toluene, THF, ether, and chloroform and are insoluble in aliphatic hydrocarbons. **2a** is appreciably soluble only in THF. None of the phosphine complexes sublimes cleanly (100-150 °C (10^{-4} mmHg)) on a preparative scale, but it was possible to obtain a mass spectrum of **2a**.[9] The latter shows a strong parent ion (P^+) multiplet as well as ion multiplets corresponding to $P - PMe_3^+$ and $P - 2PMe_3^+$.

$$W_2(TFA)_4 + 2PR_3 \xrightarrow{PhCH_3} W_2(TFA)_4 \cdot 2PR_3 \quad (2)$$
1

2a, R = Me
2b, R = Et
2c, R = *n*-Bu

The solid-state infrared spectrum (Fluorolube mulls) of each of the complexes shows two well-resolved antisymmetric C-O stretching modes, one in the region characteristic of monodentate $CF_3CO_2^-$ coordination (1652-1672 cm^{-1})[10] and one in the region characteristic of bidentate coordination (1540-1570 cm^{-1}).[10] The same band patterns are also observed in solution ($CHCl_3$ for **2b** and **2c**; THF for **2a**). For comparison, we note that the parent complex, **1**, with four bi-

(1) Presented, in part, at the 185th National Meeting of the American Chemical Society, Seattle, WA, March 1983.
(2) (a) The University of Michigan. (b) Indiana University.
(3) Sattelberger, A. P.; McLaughlin, K. W.; Huffman, J. C. *J. Am. Chem. Soc.* **1981**, *103*, 2880.
(4) (a) Cotton, F. A.; Felthouse, T. R. *Inorg. Chem.* **1981**, *20*, 3880 and references therein. (b) Cotton, F. A.; Mott, G. N.; Schrock, R. R.; Sturgeoff, L. G. *J. Am. Chem. Soc.* **1982**, *104*, 6781.
(5) Santure, D. J.; McLaughlin, K. W.; Huffman, J. C.; Sattelberger, A. P. *Inorg. Chem.* **1983**, *22*, 1877.
(6) (a) Cotton, F. A.; Wang, W. *Inorg. Chem.* **1982**, *21*, 3859. (b) Girolami, G. S.; Mainz, V. V.; Andersen, R. A. *Organometallics*, in press. (c) Chisholm, M. H., personal communication.
(7) Girolami, G. S.; Mainz, V. V.; Andersen, R. A. *Inorg. Chem.* **1980**, *19*, 805.
(8) Cotton, F. A.; Lay, D. G. *Inorg. Chem.* **1981**, *20*, 935.
(9) Instrumental limitations prevented us from looking above m/e = 1000.
(10) Garner, C. D. Hughes, B. *Adv. Inorg. Chem. Radiochem.* **1975**, *17*, 1.

0020-1669/84/1323-0938$01.50/0

Table I. Analytical and Infrared Spectral Data for Tertiary Phosphine Adducts of $W_2(TFA)_4$

complex	anal. calcd % C	anal. calcd % H	anal. found % C	anal. found % H	IR $\nu_{as}(O_2CCF_3)^a$	IR $\nu_{as}(O_2CCF_3)$
$W_2(TFA)_4 \cdot 2PMe_3$ (**2a**)	17.30	1.87	17.54	2.01	1570, 1652	1590, 1712[b]
$W_2(TFA)_4 \cdot 2PEt_3$ (**2b**)	22.74	2.86	22.59	3.00	1540, 1670	1549, 1679[c]
$W_2(TFA)_4 \cdot 2P\text{-}n\text{-}Bu_3$ (**2c**)	31.39	4.45	31.13	4.68	1549, 1677	1546, 1680[c]
$W_2(TFA)_4 \cdot 3PMe_3$ (**3**)	19.48	2.60	19.41	2.62	1565, 1585, 1665, 1710	

[a] Fluorolube mull, cm^{-1}. [b] THF solution, cm^{-1}. [c] Chloroform solution, cm^{-1}.

Table II. ^{19}F and $^{31}P\{^1H\}$ NMR Data for Tertiary Phosphine Adducts of $W_2(TFA)_4$

complex	^{19}F NMR[a,c]	$^{31}P\{^1H\}$ NMR[b,c]	coupling constants[d]
$W_2(TFA)_4 \cdot 2PMe_3$ (**2a**)	−69.8, −74.8[e]	+9.8[e]	$^1J_{PW} = 346.5$, $^2J_{PW} = 22.0$, $^3J_{PP} = 20.5$
$W_2(TFA)_4 \cdot 2PEt_3$ (**2b**)	−69.4, −75.6[f]	+19.0[f]	$^1J_{PW} = 408.1$, $^2J_{PW} = 15.7$, $^3J_{PP} = 31.7$
$W_2(TFA)_4 \cdot 2P\text{-}n\text{-}Bu_3$ (**2c**)	−69.4, −75.4[f]	+12.6[f]	$^1J_{PW} = 406.7$, $^2J_{PW} = 15.7$, $^3J_{PP} = 31.2$
$W_2(TFA)_4 \cdot 3PMe_3$ (**3**)	−69.8, −75.2,[g] −75.7, −75.8	+11.9, −17.2,[g] −19.6	$J_{AX} = 40.4$, $J_{AM} = 21.3$, $J_{MX} = 10.7$

[a] δ units relative to $CFCl_3$ (δ 0.0). [b] δ units relative to 85% H_3PO_4 (δ 0.0). [c] Negative chemical shifts correspond to resonances upfield of the reference. [d] In Hz. [e] In THF. [f] In C_6D_6. [g] In CH_2Cl_2/C_6D_6 (1:1).

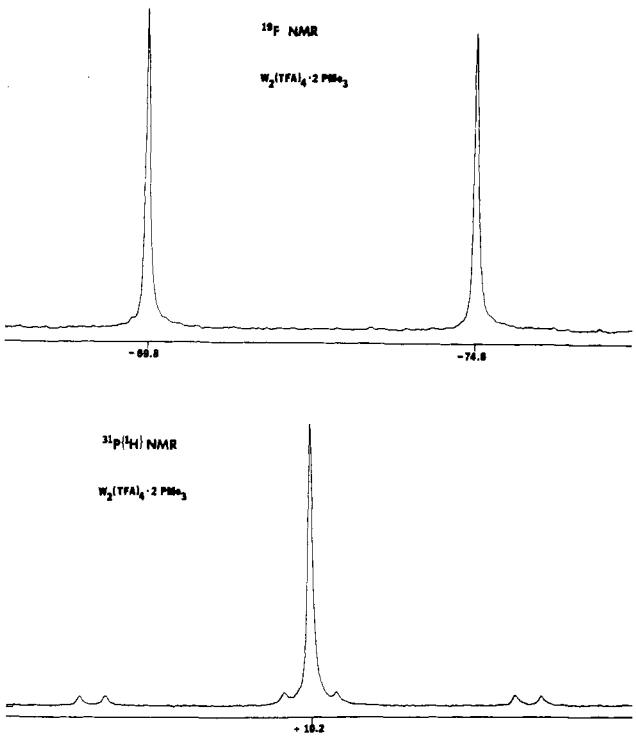

Figure 1. 84.26-MHz ^{19}F NMR (top) and 36.20-MHz $^{31}P\{^1H\}$ NMR spectra of $W_2(TFA)_4 \cdot 2PMe_3$.

dentate, bridging carboxylate ligands has its antisymmetric C–O stretching mode at 1559 cm^{-1}.[5] A tabulation of analytical and infrared spectroscopic data for **2a–c** is presented in Table I.

The room-temperature ^{19}F and $^{31}P\{^1H\}$ NMR spectra of the PMe_3 adduct, **2a**, are shown in Figure 1 and are representative of the entire series. No significant differences were observed in these spectra, or those of **2b** and **2c**, on cooling the NMR samples to −50 °C. In the ^{19}F NMR spectrum of **2a** we find two singlets, each of area 1, at δ −69.8 and −74.8 (vs. $CFCl_3$, δ 0.0). The former is indicative of bidentate $CF_3CO_2^-$ coordination[11] and the latter of monodentate carboxylate coordination.[12] The ^{19}F NMR spectrum of **1** shows a single "bidentate" resonance at δ −70.1. The $^{31}P\{^1H\}$ NMR spectrum

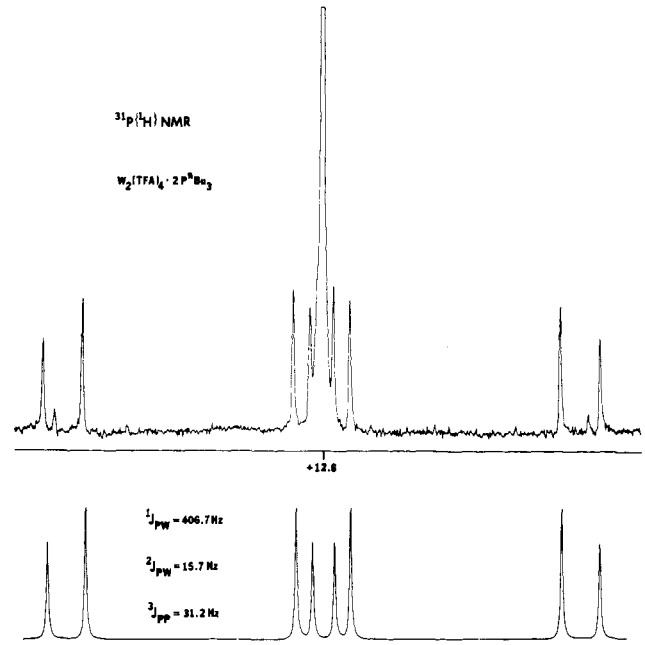

Figure 2. 36.20-MHz $^{31}P\{^1H\}$ NMR spectrum of $W_2(TFA)_4 \cdot 2P\text{-}n\text{-}Bu_3$ (top) and a computer simulation of the tungsten-183 satellite pattern (see text).

of **2a** consists of a sharp singlet at δ +10.2 (vs. 85% aqueous H_3PO_4, δ 0.0), flanked by tungsten-183 satellites. Of the five naturally occurring isotopes of tungsten, only tungsten-183 is magnetically active ($I = {}^1/_2$, 14.4% abundant). In a natural-abundance sample of $W_2(TFA)_4 \cdot 2PR_3$, 26.7% of the dimers will have a single tungsten-183 isotope in the W_2^{4+} core and 2.1% will have a $^{183}W_2^{4+}$ core. The tungsten satellite pattern in Figure 1 is characteristic of an AA′X spin system with a large AX coupling constant. This can be seen more clearly in Figure 2 (upper spectrum), where we show the $^{31}P\{^1H\}$ NMR spectrum of **2c** at higher gain. All eight of the A transitions are observed in this case, and the pattern has been simulated in the lower half of Figure 2 with use of the indicated coupling constants. A complete list of coupling constants and ^{19}F and ^{31}P NMR chemical shift data for **2a–c** is provided in Table II. There are two additional low-intensity resonances near the ends of the experimental spectrum that are unaccounted for in the computer simulation. These are the strongest A transitions of the AA′XX′ spin system $^{183}W_2(TFA)_4 \cdot 2P\text{-}n\text{-}Bu_3$, and their separation is equal to $J_{AX} + J_{A'X}$

(11) Teremoto, K.; Sasaki, Y.; Migita, K.; Iwaizumi, M.; Soito, K. *Bull. Chem. Soc. Jpn.* **1979**, *52*, 446.
(12) Dobson, A.; Robinson, S. D. *Inorg. Chem.* **1977**, *16*, 1321.

Table III. Fractional Coordinates and Isotropic Thermal Parameters for $W_2(TFA)_4 \cdot 2P\text{-}n\text{-}Bu_3$[a]

atom	x	y	z	B_{iso}, Å^2
W(1)	2302.3 (2)	1798.7 (4)	2141.0 (2)	12
O(2)	2935 (4)	117 (7)	2102 (4)	16
O(3)	2024 (4)	−558 (9)	1498 (4)	30
C(4)	2614 (6)	−677 (10)	1730 (5)	15
C(5)	3023 (7)	−1914 (11)	1597 (6)	19
F(6)	3697 (4)	−1767 (7)	1661 (4)	34
F(7)	2841 (5)	−2870 (8)	1956 (5)	50
F(8)	2882 (4)	−2298 (9)	1007 (4)	38
O(9)	1711 (4)	856 (7)	2798 (3)	13
O(10)	2908 (4)	2688 (8)	1479 (3)	15
C(11)	1745 (6)	1361 (13)	3339 (5)	18
C(12)	1362 (6)	645 (13)	3838 (5)	20
F(13)	1795 (4)	133 (9)	4268 (4)	37
F(14)	966 (4)	−296 (8)	3605 (3)	38
F(15)	946 (4)	1424 (8)	4126 (4)	40
P(16)	1311 (2)	3155 (3)	1732 (1)	15
C(17)	872 (6)	2169 (12)	1117 (5)	18
C(18)	1334 (6)	1827 (11)	591 (6)	19
C(19)	993 (6)	835 (12)	134 (6)	21
C(20)	1464 (7)	433 (14)	−357 (6)	28
C(21)	616 (6)	3661 (14)	2231 (6)	25
C(22)	172 (6)	2555 (11)	2476 (6)	21
C(23)	−425 (7)	3075 (14)	2856 (6)	28
C(24)	−164 (8)	3773 (17)	3440 (7)	36
C(25)	1558 (6)	4664 (12)	1339 (5)	18
C(26)	1001 (6)	5242 (12)	902 (6)	21
C(27)	1262 (7)	6432 (13)	568 (6)	23
C(28)	727 (7)	6946 (12)	82 (6)	26

[a] Fractional coordinates are $\times 10^4$ for non-hydrogen atoms and $\times 10^3$ for hydrogen atoms. B_{iso} values are $\times 10$. Isotropic values for those atoms refined anisotropically are calculated by using the formula given by: Hamilton, W. C. *Acta Crystallogr.* 1959, *12*, 609.

or $^1J_{PW} + {}^2J_{PW}$. We already know the latter sum from our analysis of the AA'X spin system, and the agreement between the observed and calculated separations (both 422 Hz) confirms the assignment. Regrettably, we were unable to resolve the eight remaining A transitions; they would have provided $^1J_{WW}$, an unknown quantity for any binuclear tungsten complex.

The solution NMR data on **2a–c** provides two important pieces of information: (1) we are dealing with a single equatorial isomer in each case, and (2) the phosphine ligands in these complexes must be on adjacent metal centers. The ^{31}P NMR data do not, a priori, provide information on the stereochemistry of the phosphines. From steric considerations, we would predict that these ligands are trans to each other across the tungsten–tungsten bond, i.e., a P–W–W–P torsion angle of 180°, but we do not, at this state in the development of W≡W chemistry, know how $^3J_{PP}$, for a given phosphine, varies as a function of the P–W–W–P torsion angle *or* the metal–metal bond length. All we can say at this point is that the NMR data are consistent with what we perceive is the thermodynamically most stable equatorial isomer. Since the solution and solid-state infrared spectra of **2a–c** are similar, an X-ray structure of one member of the series should resolve the spectroscopic ambiguity inherent in the NMR data. We provide this information in the next section.

The simplicity of the solution behavior of **2a–c** contrasts sharply with that exhibited by equatorial $Mo_2(TFA)_4 \cdot 2L$ complexes.[7] In the cases where L = PEt_3 or PMe_2Ph, the presence of two equatorial isomers in the $CDCl_3$ solutions of each is required to explain the −55 °C $^{31}P\{^1H\}$ NMR spectra.[13] The situation when L = PMe_3 is more complex. At −11 °C in $CDCl_3$, two types of phosphine environments are observed, but at −55 °C,[13] the presence of five different equatorial isomers is required to explain the five $^{31}P\{^1H\}$ NMR resonances at δ −4.59, −6.03, −7.03, −8.16, and −10.0 (area ratios 5:3:1:4:1). Why is the solution behavior of equatorial $Mo_2(TFA)_4 \cdot 2L$ and $W_2(TFA)_4 \cdot 2L$ complexes so different? Let us examine the structure of **2c** to see if its provides any clues.

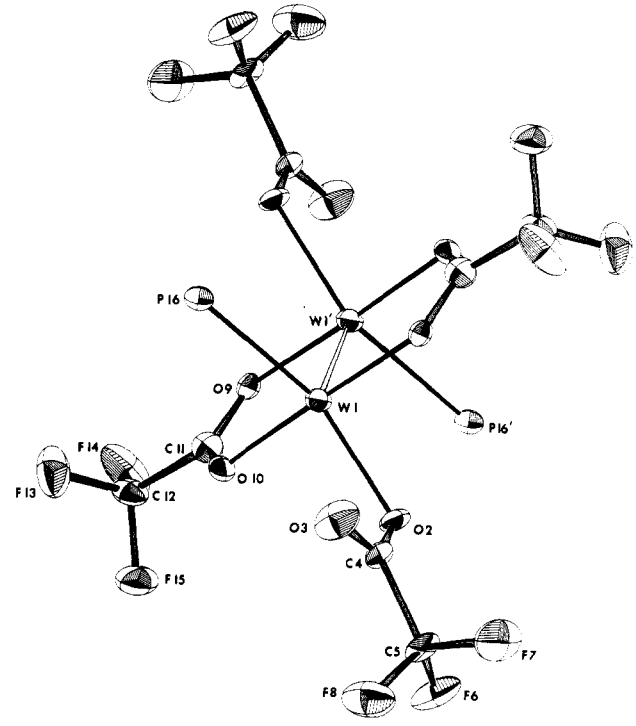

Figure 3. ORTEP drawing of $W_2(TFA)_4 \cdot 2P\text{-}n\text{-}Bu_3$ with the *n*-butyl groups deleted. The molecule resides on a center of symmetry.

Solid-State Structure of $W_2(TFA)_4 \cdot 2P\text{-}n\text{-}Bu_3$ (2c). Crystal data for **2c** is provided in the Experimental Section. Positional and isotropic thermal parameters are presented in Table III, and selected interatomic distances and angles are given in Table IV. In the space group $I2/a$ (a nonstandard setting of the monoclinic space group $C2/c$) with $Z = 4$, crystallographic inversion symmetry is imposed on **2c**. An ORTEP drawing of the dimer is shown in Figure 3. We have deleted the ordered *n*-butyl groups on phosphorus so that the inner core can be seen more clearly. The point symmetry of the latter, i.e., the two tungsten and eight ligand atoms, is approximately C_{2h}.

The important structural features of **2c** include the following: (1) a tungsten–tungsten bond length of 2.224 (1) Å, which is midway between the W≡W bond lengths found in the *axial* diglyme (2.209 [2] Å) and triphenylphosphine (2.242 [2] Å) adducts of **1**; (2) a tungsten–phosphorus bond length of 2.489 (3) Å and a W–W–P bond angle of 95.7 (1)°; (3) tungsten–oxygen bond lengths of 2.132 (7) and 2.107 (7) Å and W–W–O bond angles of 113.0 (2) and 90.5 (3)° for the monodentate and bidentate carboxylates, respectively; (4) a weak axial interaction between the tungstens and the carbonyl oxygens of the monodentate $CF_3CO_2^-$ groups (W(1)···O(3) = 2.845 (8) Å; W(1)'–W(1)–O(3) = 161.3 (2)°).

Structural data on the molybdenum homologue of **2c** are not available at this time, but there are two equatorial adducts of $Mo_2(TFA)_4$ that have been characterized by X-ray diffraction. In $Mo_2(TFA)_4 \cdot 2PEt_2Ph$[8] and $Mo_2(TFA)_4 \cdot 2PMePh_2$,[8,14] both of which have the same phosphine stereo-

(13) We assume that these temperatures correspond to the stopped-exchange region.

(14) (a) An axial isomer of $Mo_2(TFA)_4 \cdot 2PMePh_2$ has also been structurally characterized.[14b] (b) Girolami, G. S.; Andersen, R. A. *Inorg. Chem.* **1982**, *21*, 1318.

Table IV. Selected Bond Distances (Å) and Angles (deg) for $W_2(TFA)_4 \cdot 2P\text{-}n\text{-}Bu_3$

A	B	dist
W(1)	W(1)	2.224 (1)
W(1)	P(16)	2.489 (3)
W(1)	O(2)	2.132 (7)
W(1)	O(9)	2.107 (7)
W(1)	O(10)	2.106 (8)
P(16)	C(17)	1.839 (12)
P(16)	C(21)	1.841 (12)
P(16)	C(25)	1.854 (12)
F(6)	C(5)	1.306 (15)
F(7)	C(5)	1.318 (15)
F(8)	C(5)	1.345 (15)
F(13)	C(12)	1.320 (14)
F(14)	C(12)	1.320 (14)
F(15)	C(12)	1.317 (14)
O(2)	C(4)	1.282 (14)
O(3)	C(4)	1.218 (14)
O(9)	C(11)	1.276 (14)
O(10)	C(11)	1.242 (15)
C(4)	C(5)	1.541 (15)
C(11)	C(12)	1.529 (17)
C(17)	C(18)	1.523 (17)
C(18)	C(19)	1.541 (17)
C(19)	C(20)	1.492 (18)
C(21)	C(22)	1.542 (19)
C(22)	C(23)	1.544 (18)
C(23)	C(24)	1.512 (21)
C(25)	C(26)	1.508 (17)
C(26)	C(27)	1.528 (18)
C(27)	C(28)	1.520 (19)

A	B	C	angle
W(1)	W(1)	P(16)	95.7 (1)
W(1)	W(1)	O(2)	113.0 (2)
W(1)	W(1)	O(9)	90.8 (2)
W(1)	W(1)	O(10)	90.2 (2)
P(16)	W(1)	O(2)	151.2 (2)
P(16)	W(1)	O(9)	93.9 (2)
P(16)	W(1)	O(10)	87.4 (2)
O(2)	W(1)	O(9)	88.8 (3)
O(2)	W(1)	O(10)	89.6 (3)
O(9)	W(1)	O(10)	178.3 (3)
W(1)	P(16)	C(17)	104.5 (4)
W(1)	P(16)	C(21)	121.5 (5)
W(1)	P(16)	C(25)	115.3 (4)
C(17)	P(16)	C(21)	105.0 (5)
C(17)	P(16)	C(25)	105.2 (5)
C(21)	P(16)	C(25)	103.9 (6)
W(1)	O(2)	C(4)	107.2 (7)
W(1)	O(9)	C(11)	115.0 (7)
W(1)	O(10)	C(11)	116.4 (7)
O(2)	C(4)	O(3)	126.4 (11)
O(2)	C(4)	C(5)	114.7 (10)
O(3)	C(4)	C(5)	118.8 (10)
F(6)	C(5)	F(7)	108.9 (11)
F(6)	C(5)	F(8)	106.0 (10)
F(6)	C(5)	C(4)	113.5 (9)
F(7)	C(5)	F(8)	106.6 (10)
F(7)	C(5)	C(4)	111.3 (10)
F(8)	C(5)	C(4)	110.2 (10)
O(9)	C(11)	O(10)	127.7 (11)
O(9)	C(11)	C(12)	116.2 (11)
O(10)	C(11)	C(12)	115.9 (10)
F(13)	C(12)	F(14)	107.1 (11)
F(13)	C(12)	F(15)	107.0 (10)
F(13)	C(12)	C(11)	112.2 (9)
F(14)	C(12)	F(15)	106.2 (9)
F(14)	C(12)	C(11)	112.6 (10)
F(15)	C(12)	C(11)	111.3 (11)
P(16)	C(17)	C(18)	113.7 (8)
C(17)	C(18)	C(19)	112.7 (10)
C(18)	C(19)	C(20)	112.7 (11)
P(16)	C(21)	C(22)	115.1 (9)
C(21)	C(22)	C(23)	111.4 (10)
C(22)	C(23)	C(24)	112.8 (11)
P(16)	C(25)	C(26)	115.4 (8)
C(25)	C(26)	C(27)	112.0 (10)
C(26)	C(27)	C(28)	112.4 (11)

chemistry as **2c**, the Mo$\frac{4}{-}$Mo bond lengths are 2.100 (1) and 2.107 (2) Å and the Mo–P bond lengths are 2.532 (1) and 2.511 (3) Å, respectively. The difference between Mo$\frac{4}{-}$Mo and W$\frac{4}{-}$W bond lengths in these equatorial adducts (ca. 0.12 Å) is not very surprising since in all previously reported cases of homologous or closely related molybdenum and tungsten quadruply bonded complexes, the W$\frac{4}{-}$W bonds are appreciably longer (by 0.073 (2)[15] to 0.132 (2) Å[16]). The lengthening of M–P bonds as one goes from **2c** to the two equatorial adducts of $Mo_2(TFA)_4$ is not unexpected either. In the $M_2Cl_4(PMe_3)_4$ dimers (trans PMe_3),[16] for example, the Mo–P bonds are 0.038 (2) Å longer than their tungsten counterparts (W–P = 2.508 [2] Å). It would appear, from the admittedly sparse structural data available, that equatorial Mo–P bonds are inherently longer and weaker than equatorial W–P bonds.[17] Whether this is a reflection of stronger M–P σ bonding, an increase in $d\pi$–$d\pi$ back-bonding (via the δ and π metal–metal bond orbitals), or a combination of both in the ditungsten systems is not entirely clear at the present time. Regardless of one's prejudices on this point, the fact remains that, aside from an increase in M$\frac{4}{-}$M bond length (Mo → W), the only substantive structural difference in the three $M_2(TFA)_4 \cdot 2PR_3$ complexes under consideration here is in the M–P bond lengths. It is likely that the differences in solution behavior between $Mo_2(TFA)_4 \cdot 2L$ (L = PMe_3, PEt_3, PMe_2Ph) and **2a–c** are a direct reflection of the differences in M–P bond strengths. The connection between weak Mo–P bonds and the observation of two (or more) equatorial molybdenum isomers in solution will be the subject of another paper in this series.[17c,18]

Synthesis and Physicochemical Properties of $W_2(TFA)_4 \cdot 3PMe_3$. Toluene solutions of **1** or toluene suspensions of **2a** react rapidly with trimethylphosphine to provide dark green $W_2(TFA)_4 \cdot 3PMe_3$ (**3**), according to eq 3 and 4. This air-

$$\underset{\mathbf{1}}{W_2(TFA)_4} + 3PMe_3 \xrightarrow{PhCH_3} \underset{\mathbf{3}}{W_2(TFA)_4 \cdot 3PMe_3} \quad (3)$$

$$\underset{\mathbf{2a}}{W_2(TFA)_4 \cdot 2PMe_3} + PMe_3 \xrightarrow{PhCH_3} \underset{\mathbf{3}}{W_2(TFA)_4 \cdot 3PMe_3} \quad (4)$$

sensitive tris(phosphine) adduct is stable in solution ($PhCH_3$ or CH_2Cl_2), in the absence of free PMe_3, at 25 °C. Thermolysis of **3** (PhH, 50 °C, 30 min) provides a red precipitate whose solution (THF) NMR properties are identical with those of **2a** (eq 5). The infrared spectrum of **3** (Fluorolube mull)

$$\underset{\mathbf{3}}{W_2(TFA)_4 \cdot 3PMe_3} \xrightarrow[PhH]{\Delta} \underset{\mathbf{2a}}{W_2(TFA)_4 \cdot 2PMe_3} + PMe_3 \quad (5)$$

shows four antisymmetric C–O stretching modes at 1710, 1665, 1585, and 1565 cm^{-1}. The first pair are assigned to

(15) Cotton, F. A.; Koch, S. A.; Schultz, A. J.; Williams, J. M. *Inorg. Chem.* **1978**, *17*, 2093.

(16) Cotton, F. A.; Extine, M. W.; Felthouse, T. R.; Kolthammer, B. W. S.; Lay, D. G. *J. Am. Chem. Soc.* **1981**, *103*, 4040.

(17) (a) The covalent radii of molybdenum and tungsten are virtually identical,[17b] and as such, the terms longer and weaker are synonymous. In the three $M_2(TFA)_4 \cdot 2L$ complexes whose structures have been determined, the differences in M–O bond lengths are statistically insignificant but the differences in M–P bond lengths are significant. It is unfortunate that we do not have the structure of $Mo_2(TFA)_4 \cdot 2P\text{-}n\text{-}Bu_3$ for comparison.[17c] We think it will have an even longer Mo–P bond length than either the PEt_2Ph or the $PMePh_2$ complex. (b) Cotton, F. A.; Wilkinson, G. "Advanced Inorganic Chemistry", 4th ed.; Wiley: New York, 1980; pp 822–823. (c) We have prepared this complex by the same methods used for **2c**. Its low melting point thwarted our efforts to collect a room-temperature X-ray data set. We hope to collect low-temperature data in the near future.

(18) From the available data[7,8,14b] on $Mo_2(TFA)_4 \cdot 2L$ complexes, it is unclear whether the isomerization process is intra- or intermolecular. We suspect the latter, but several key experiments, e.g., $Mo_2(TFA)_4 \cdot 2L + Mo_2(TFA)_4 \cdot 2L'$, must be done to confirm this. This work is in progress.

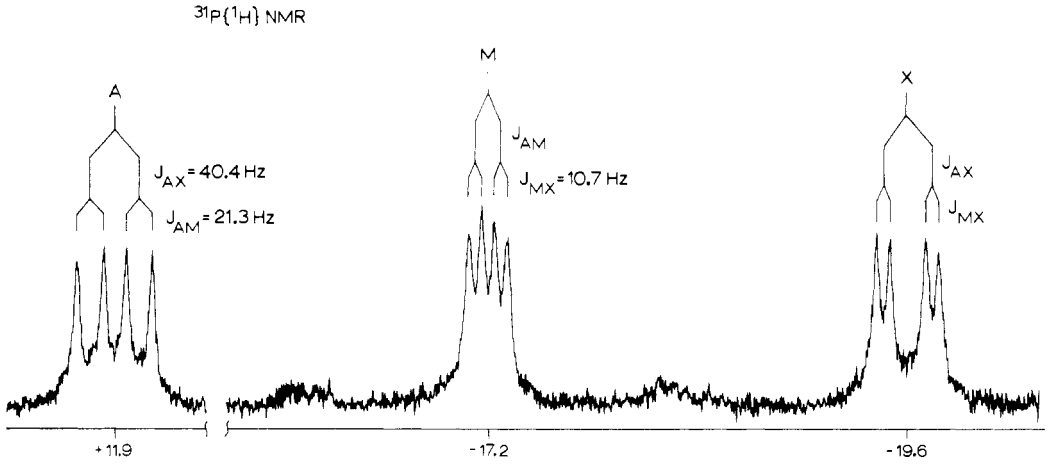

Figure 4. 145.8-MHz $^{31}P\{^1H\}$ NMR spectrum of $W_2(TFA)_4 \cdot 3PMe_3$.

monodentate $CF_3CO_2^-$ groups and the second pair to the unique bidentate carboxylate ligand (vide infra).

The room-temperature ^{19}F NMR spectrum of **3** shows four singlets, each of area 1, at δ −69.8, −75.2, −75.7, and −75.8. Only the first of these can be assigned as a bidentate trifluoroacetate ligand, which means that the third phosphine occupies an equatorial site in the dimer framework.

In the $^{31}P\{^1H\}$ NMR spectrum of **3** (Figure 4), we observe three resonances, each with approximately the same integrated intensity, at δ +11.2, −17.2, and −19.6. The observed splitting pattern is characteristic of an AMX spin system, and the coupling constants that define the present case are indicated in Figure 4.

Collectively, the IR and NMR data define the structure of **3** as C, which is essentially that found by less sporting methods that we describe in the next section.

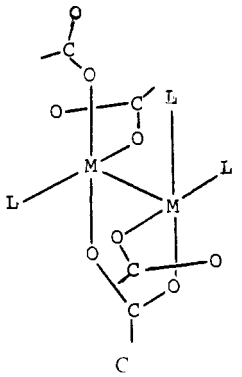

C

Solid-State Structure of $W_2(TFA)_4 \cdot 3PMe_3$ (3). Crystal data for **3** are provided in the Experimental Section. Positional and isotropic thermal parameters are presented in Table V, and selected interatomic distances and angles are given in Table VI. In acentric orthorhombic space group $Pc2_1n$ (an alternate setting of $Pna2_1$) with Z = 4, no crystallographic symmetry is imposed on **3**. An ORTEP drawing of the molecule is shown in Figure 5. We have deleted the phosphine methyl groups from the drawing so that the inner core is visible. The solid-state structure is in total accord with the spectroscopic data. There are three chemically nonequivalent, monodentate carboxylate ligands (one on W(1), two on W(2)), three chemically nonequivalent PMe_3 ligands (two on W(1), one on W(2)), and a single bidentate trifluoroacetate bridging W(1) and W(2). Note that the addition of a PMe_3 ligand to **2a** provides a chiral product in which there is a formal oxidation-state difference between the two tungsten atoms: W(1) = +1.5 and W(2) = +2.5.

The important structural features of **3** include the following: (1) The tungsten–tungsten bond length is 2.246 (1) Å, which is 0.022 (1) Å longer than that found in **2c**. (2) Tungsten–phosphorus bond lengths are 2.462 (5), 2.492 (5), and 2.504 (5) Å for W(1)–P(3), W(2)–P(11), and W(1)–P(7), respectively. The corresponding W–W–P bond angles are 93.5 (1),

Table V. Fractional Coordinates and Isotropic Thermal Parameters for $W_2(TFA)_4 \cdot 3PMe_3$[a]

atom	x	y	z	B_{iso}, Å^2
W(1)	−4907 (1)	0*	3911.9 (3)	13
W(2)	−3222 (1)	745 (1)	3431.1 (3)	15
P(3)	−4510 (5)	−1372 (3)	3299 (3)	19
C(4)	−5587 (22)	−2246 (14)	3639 (11)	29
C(5)	−2858 (22)	−1873 (15)	3380 (11)	33
C(6)	−4812 (26)	−1460 (17)	2461 (11)	37
P(7)	−6938 (5)	499 (3)	3297 (3)	22
C(8)	−7291 (26)	1646 (16)	3342 (14)	43
C(9)	−7086 (19)	327 (21)	2455 (10)	43
C(10)	−8449 (21)	−38 (26)	3594 (14)	59
P(11)	−3241 (5)	2019 (4)	4188 (2)	19
C(12)	−4733 (20)	2743 (15)	4252 (10)	27
C(13)	−2804 (18)	1727 (15)	4975 (10)	24
C(14)	−1888 (30)	2766 (18)	3973 (11)	47
O(15)	−5778 (11)	721 (10)	4676 (5)	18
O(16)	−6673 (13)	−584 (9)	4888 (6)	20
C(17)	−6565 (18)	207 (12)	4984 (9)	22
C(18)	−7363 (18)	652 (14)	5509 (10)	26
F(19)	−6932 (12)	101 (11)	5906 (6)	37
F(20)	−8397 (12)	1126 (10)	5239 (7)	49
F(21)	−6648 (13)	1233 (10)	5847 (7)	49
O(22)	−3535 (11)	−532 (8)	4573 (6)	16
O(23)	−1864 (11)	158 (10)	4046 (6)	22
C(24)	−2298 (19)	−345 (12)	4504 (10)	20
C(25)	−1285 (19)	−744 (14)	4935 (8)	19
F(26)	−1768 (15)	−1373 (15)	5279 (10)	79
F(27)	−884 (23)	−202 (13)	5354 (11)	105
F(28)	−210 (18)	−1041 (18)	4671 (8)	92
O(29)	−4086 (12)	1412 (9)	2678 (6)	19
O(30)	−3192 (16)	2763 (10)	2516 (8)	37
C(31)	−3784 (18)	2101 (14)	2344 (9)	19
C(32)	−4212 (18)	1973 (15)	1667 (9)	23
F(33)	−4040 (14)	2698 (9)	1304 (6)	40
F(34)	−5487 (13)	1717 (12)	1599 (6)	53
F(35)	−3443 (15)	1357 (11)	1384 (6)	47
O(36)	−2373 (13)	−35 (10)	2693 (6)	24
O(37)	−845 (12)	1022 (10)	2493 (6)	25
C(38)	−1413 (18)	305 (13)	2370 (9)	18
C(39)	−915 (18)	−246 (14)	1816 (12)	31
F(40)	−556 (36)	218 (15)	1367 (10)	146
F(41)	35 (23)	−744 (21)	1976 (12)	127
F(42)	−1843 (16)	−754 (16)	1598 (9)	85

[a] Fractional coordinates are $\times 10^4$ for non-hydrogen atoms and $\times 10^3$ for hydrogen atoms. B_{iso} values are $\times 10$. Isotropic values for those atoms refined anisotropically are calculated by using the formula given by: Hamilton, W. C. *Acta Crystallogr.* 1959, *12*, 609. Parameters marked by an asterisk were not varied.

Table VI. Selected Bond Distances (Å) and Angles (deg) for $W_2(TFA)_4 \cdot 3PMe_3$

A	B	dist	A	B	dist
W(1)	W(2)	2.246 (1)	F(26)	C(25)	1.283 (25)
W(1)	P(3)	2.462 (5)	F(27)	C(25)	1.266 (24)
W(1)	P(7)	2.504 (5)	F(28)	C(25)	1.278 (23)
W(1)	O(15)	2.124 (12)	F(33)	C(32)	1.342 (24)
W(1)	O(22)	2.101 (11)	F(34)	C(32)	1.324 (22)
W(2)	P(11)	2.492 (5)	F(35)	C(32)	1.337 (24)
W(2)	O(23)	2.064 (12)	F(40)	F(42)	1.995 (31)
W(2)	O(29)	2.064 (13)	F(40)	C(39)	1.230 (29)
W(2)	O(36)	2.121 (13)	F(41)	C(39)	1.245 (30)
P(3)	C(4)	1.835 (19)	F(42)	C(39)	1.278 (25)
P(3)	C(5)	1.804 (22)	O(15)	C(17)	1.273 (22)
P(3)	C(6)	1.799 (22)	O(16)	C(17)	1.208 (24)
P(7)	C(8)	1.758 (24)	O(22)	C(24)	1.262 (21)
P(7)	C(9)	1.801 (23)	O(23)	C(24)	1.298 (23)
P(7)	C(10)	1.807 (24)	O(29)	C(31)	1.286 (23)
P(11)	C(12)	1.835 (22)	O(30)	C(31)	1.209 (24)
P(11)	C(13)	1.771 (22)	O(36)	C(38)	1.275 (22)
P(11)	C(14)	1.802 (26)	O(37)	C(38)	1.240 (24)
F(19)	C(18)	1.305 (24)	C(17)	C(18)	1.515 (26)
F(20)	C(18)	1.368 (23)	C(24)	C(25)	1.479 (28)
F(21)	C(18)	1.330 (24)	C(31)	C(32)	1.503 (28)
F(26)	F(27)	1.967 (30)	C(38)	C(39)	1.514 (28)

A	B	C	angle	A	B	C	angle
W(2)	W(1)	P(3)	93.5 (1)	C(5)	P(3)	C(6)	102.3 (11)
W(2)	W(1)	P(7)	102.1 (1)	W(1)	P(7)	C(8)	115.0 (9)
W(2)	W(1)	O(15)	112.9 (3)	W(1)	P(7)	C(9)	122.3 (8)
W(2)	W(1)	O(22)	90.7 (3)	W(1)	P(7)	C(10)	110.3 (10)
P(3)	W(1)	P(7)	96.0 (2)	C(8)	P(7)	C(9)	100.2 (14)
P(3)	W(1)	O(15)	152.8 (4)	C(8)	P(7)	C(10)	104.7 (15)
P(3)	W(1)	O(22)	86.0 (4)	C(9)	P(7)	C(10)	102.2 (12)
P(7)	W(1)	O(15)	85.3 (3)	W(2)	P(11)	C(12)	120.5 (7)
P(7)	W(1)	O(22)	166.9 (3)	W(2)	P(11)	C(13)	114.2 (7)
O(15)	W(1)	O(22)	87.1 (5)	W(2)	P(11)	C(14)	108.0 (8)
W(1)	W(2)	P(11)	94.9 (1)	C(12)	P(11)	C(13)	105.8 (9)
W(1)	W(2)	O(23)	89.1 (4)	C(12)	P(11)	C(14)	104.2 (12)
W(1)	W(2)	O(29)	106.5 (3)	C(13)	P(11)	C(14)	102.2 (11)
W(1)	W(2)	O(36)	110.5 (4)	F(27)	F(26)	C(25)	39.2 (12)
P(11)	W(2)	O(23)	85.9 (4)	F(26)	F(27)	C(25)	39.8 (12)
P(11)	W(2)	O(29)	96.9 (4)	F(42)	F(40)	C(39)	38.1 (15)
P(11)	W(2)	O(36)	153.8 (4)	F(40)	F(42)	C(39)	36.4 (16)
O(23)	W(2)	O(29)	163.8 (5)	W(1)	O(15)	C(17)	109.1 (12)
O(23)	W(2)	O(36)	88.3 (5)	W(1)	O(22)	C(24)	117.5 (11)
O(29)	W(2)	O(36)	82.2 (5)	W(2)	O(23)	C(24)	120.1 (11)
W(1)	P(3)	C(4)	107.4 (7)	W(2)	O(29)	C(31)	135.8 (12)
W(1)	P(3)	C(5)	116.2 (8)	W(2)	O(36)	C(38)	117.8 (13)
W(1)	P(3)	C(6)	123.5 (8)	O(15)	C(17)	O(16)	124.3 (19)
C(4)	P(3)	C(5)	100.9 (11)	O(15)	C(17)	C(18)	115.1 (16)
C(4)	P(3)	C(6)	103.7 (12)	O(16)	C(17)	C(18)	120.6 (18)

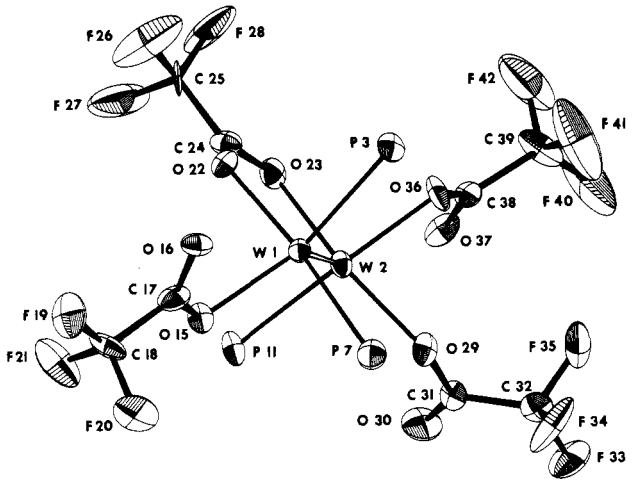

Figure 5. ORTEP drawing of $W_2(TFA)_4 \cdot 3PMe_3$ with the phosphine methyl groups deleted.

94.9 (1), and 102.1 (1)°; i.e., the shortest W–P bond is associated with the most acute W–W–P bond angle and so forth.

(3) The angle between the cis phosphines on W(1) (i.e., P(3)–W(1)–P(7)) is 96.0 (2)°, and the torsion angles, P(3)–W(1)–W(2)–P(11) and P(7)–W(1)–W(2)–P(11), are −168.5 and +96.9°, respectively. (4) The trans influence of the PMe_3 ligands on W–O bond lengths in **3** is apparent when we compare those W–O bonds that are opposite the three phosphines with the pair of W–O bonds that are trans to each other. The former are 0.04–0.06 (1) Å longer than W(2)–O(23) or W(2)–O(29), both of which are 2.06 (1) Å. (5) There are weak axial interactions with two of the monodentate carboxylate ligands. The W(1)···O(16) contact is 2.84 (1) Å, and the W(2)···O(37) contact is 3.10 (1) Å; the W(2)–W(1)–O(16) and W(1)–W(2)–O(37) angles are 159.5 (4) and 156.4 (4)°, respectively.

A tris(trimethylphosphine) adduct of $Mo_2(TFA)_4$ is also known,[7] but it has not been characterized by X-ray diffraction. A comparison of its solid-state IR[7] and solution NMR spectra[19] with those of **3** suggests that the $M_2(TFA)_4 \cdot 3PMe_3$ complexes of molybdenum and tungsten are isostructural.

(19) Girolami, G. S. Ph.D. Thesis, University of California, Berkeley, CA, 1981.

Their solution behavior provides further evidence of the difference in M–P bond strengths as we move down the periodic table. As noted above, **3** is stable in solution at 25 °C in the absence of free phosphine. $Mo_2(TFA)_4 \cdot 3PMe_3$, on the other hand, can be observed in solution only when excess PMe_3 is present.[19]

Summary. The following are the principal results and conclusions of this investigation.

(i) $W_2(TFA)_4$, as advertised,[5] forms 1:2 equatorial adducts, $W_2(TFA)_4 \cdot 2PR_3$, with small basic tertiary phosphines.

(ii) In solution, only one of six possible equatorial isomers[7] can be detected and a C_{2h} core structure is assigned to it.

(iii) The X-ray structure of $W_2(TFA)_4 \cdot 2P\text{-}n\text{-}Bu_3$ confirms this stereochemistry and reveals a comparatively short W–P bond length of 2.489 (3) Å.

(iv) An equatorial trisadduct, $W_2(TFA)_4 \cdot 3PMe_3$, has been isolated and structurally characterized. Its structural integrity is also maintained in solution.

(v) The differences in solution behavior between $Mo_2(TFA)_4 \cdot 2PR_3$ and $W_2(TFA)_4 \cdot 2PR_3$ and between $Mo_2(TFA)_4 \cdot 3PMe_3$ and $W_2(TFA)_4 \cdot 3PMe_3$ are suggested to arise from differences in the M–P bond strengths: W–P > Mo–P.

Experimental Section

Reagents. $W_2(TFA)_4$ was prepared as described elsewhere[5] and resublimed for the reactions described below. Trimethylphosphine was prepared by the method of Wolfsberger and Schmidbaur.[20] Triethyl- and tri-*n*-butylphosphine were obtained from Orgmet and used without further purification.

Toluene and THF were dried and freed from dissolved molecular oxygen by distillation from a solution of the solvent, benzophenone, and sodium or potassium. Hexane was distilled from a solution containing *n*-butyllithium. Solvents were stored in 500-mL bottles inside our Vacuum Atmospheres HE-43 drybox. The latter is equipped with a high-capacity purification train (MO-40V) and a Dri-Cold freezer operating at −40 °C. Benzene-d_6 was dried and stored over freshly cut sodium in the drybox.

Physical and Analytical Measurements. Elemental analyses were performed by Galbraith Laboratories, Knoxville, TN, and Schwarzkopf Microanalytical Laboratory, Woodside, NY.

Infrared measurements were obtained from Nujol mulls or solutions ($CHCl_3$ and THF) between KBr plates with a Perkin-Elmer Model 1330 infrared spectrometer. Samples were prepared in the drybox and run immediately to prevent aerial oxidation.

NMR spectra were obtained on JEOL FX90Q and Bruker WM 360 spectrometers. ^{19}F spectra were recorded at 84.26 MHz, ^{31}P spectra at 36.20 or 145.80 MHz, and ^1H spectra at 360.1 MHz. Benzene-d_6 was used as a lock solvent for most spectra. The ^{19}F and $^{31}P\{^1H\}$ spectra of **2a** were run on external lock. Fluorine and phosphorus chemical shifts (δ) are reported relative to external $CFCl_3$ and 85% aqueous H_3PO_4, both of which are assigned a δ value of 0.0. Negative chemical shifts are assigned to resonances at lower frequency (higher field) than the reference materials. The computer simulations in Figure 2 were obtained on our Bruker WM360 using the Bruker PANIC NMR simulation and iteration program.

Mass spectra were obtained on a Finnegan mass spectrometer by the method of direct insertion. A probe temperature of 100–200 °C and ionizing voltages of 40–70 eV were employed. Instrumental limitations prevented us from looking above m/e = 1000. Isotope patterns were calculated by using a local program written by Steve Werness of the Chemistry Department at The University of Michigan.

General Procedures. Due to the oxidative instability of $W_2(TFA)_4$, its derivatives, and the tertiary phosphines, all preparations and manipulations were carried out under dry and oxygen-free conditions with use of Schlenk or drybox techniques.

$W_2(TFA)_4 \cdot 2PMe_3$ (2a). Trimethylphosphine (0.185 g, 2.43 mmol) was added, with a calibrated syringe, to a stirred solution of $W_2(TFA)_4$ (1.0 g, 1.22 mmol) in 20 mL of toluene at 0 °C under N_2 or He (drybox atmosphere). The bright yellow tungsten carboxylate solution immediately turned a deep red, and red solid precipitated. After 10 min the suspension was filtered and the red solid was washed with toluene (2 × 5 mL) and hexane (2 × 5 mL) and then dried in vacuo; yield 0.95 g, 80%. This material was analytically and spectroscopically pure.

$W_2(TFA)_4 \cdot 2PEt_3$ (2b). Triethylphosphine (0.288 g, 2.44 mol) was added to a stirred solution of $W_2(TFA)_4$ (1.0 g, 1.22 mmol) in 20 mL of toluene at 25 °C under N_2 or He. The solution immediately turned red. After 10 min, the volume was reduced until a precipitate appeared. At this point the suspension was placed in the freezer (−40 °C) to complete the precipitation. After 12 h, the red-orange crystalline material was filtered off, washed with hexane (3 × 5 mL), and dried in vacuo. A second recrystallization from toluene/hexane at −40 °C provided analytically and spectroscopically pure material; yield 1.06 g, 82%.

$W_2(TFA)_4 \cdot 2P\text{-}n\text{-}Bu_3$ (2c). This red-orange crystalline material was prepared in the same manner as **2b**; yield 75%.

$W_2(TFA)_4 \cdot 3PMe_3$ (3). Trimethylphosphine (0.38 g, 5 mmol, excess) was added to a stirred solution of $W_2(TFA)_4$ (0.50 g, 0.61 mmol) in 15 mL of toluene at 0 °C under N_2 or He. The solution turns deep green. After 15 min of stirring at room temperature, the solution was cooled to −40 °C overnight. The deep green crystalline solid was then filtered off, washed with hexane (2 × 5 mL), and dried in vacuo; yield 0.30 g, 45%.

3 can also be prepared from **2a** and excess phosphine. The workup is identical.

^1H NMR (ppm, C_6D_6, 360.1 MHz): 1.21, 1.24 (overlapping doublets, 2, J_{PH} = 8.3, 9.8 Hz, respectively); 1.00 (d, 1, J_{PH} = 9.5 Hz).

X-ray Structure Determinations. General procedures used were the same as those described in detail elsewhere.[21] Crystal data are summarized in Table VII.

$W_2(TFA)_4 \cdot 2P\text{-}n\text{-}Bu_3$. X-ray-quality crystals were obtained by slow cooling of hot, concentrated hexane solutions. Inside a nitrogen-filled drybag, a well-formed, red-orange block was mounted on a glass fiber with silicon grease and transferred to the liquid-nitrogen boil-off cooling system of the diffractometer. A systematic search of the reciprocal lattice revealed a centered monoclinic lattice. Due to the acute β angle the nonstandard setting $I2/a$ was chosen.[22] Diffraction data were

Table VII. Crystal Data for $W_2(TFA)_4$ Phosphine Adducts

	$W_2(TFA)_4 \cdot 2P\text{-}n\text{-}Bu_3$	$W_2(TFA)_4 \cdot 3PMe_3$
mol formula	$C_{32}H_{54}F_{12}O_8P_2W_2$	$C_{17}H_{27}F_{12}O_8P_3W_2$
color	red-orange	dark green
cryst dimens, mm	0.09 × 0.12 × 0.16	0.04 × 0.05 × 0.05
space group	$I2/a$	$Pc2_1n$
cell dimens		
temp, °C	−162	−163
a, Å	19.240 (6)	9.870 (3)
b, Å	10.379 (2)	15.002 (6)
c, Å	21.522 (2)	21.118 (10)
β, deg	93.39 (2)	
molecules/cell	4	4
cell vol, Å^3	1224.40	3126.87
d(calcd), g cm^{-3}	1.896	2.226
wavelength, Å	0.710 69	0.710 69
mol wt	1224.40	1048.00
linear abs coeff, cm^{-1}	56.406	77.683
max abs	0.352	
min abs	0.266	
diffractometer	Picker 4-circle	Picker 4-circle
mode	θ–2θ	θ–2θ
2θ range, deg	6–45	6–45
quadrants collected	$+h,+k,\pm l$	$+h,+k,+l$
no. of data with $F_o > 2.33\sigma(F_o)$	2514	1841
no. of unique data	2813	2002
total data collected	3693	2114
agreement for equiv data	0.016	0.023
final residuals		
R_F	0.042	0.036
R_{wF}	0.037	0.035
goodness of fit, last cycle	3.390	1.021
max Δ/σ, last cycle	0.05	0.05

(20) Wolfsberger, W.; Schmidbaur, H. *Synth. React. Inorg. Met.-Org. Chem.* **1974**, *4*, 149.

(21) Huffman, J. C.; Lewis, L. N.; Caulton, K. G. *Inorg. Chem.* **1980**, *19*, 2755.

collected at −162 ± 4 °C, and the structure was solved by direct methods and Fourier techniques. Statistical tests and the successful solution and refinement[23] indicate the centrosymmetric space group to be correct. ψ scans of several reflections were not flat, so an analytical absorption correction was applied. All atoms, with the exception of the butyl group hydrogens, were located and their positional and thermal parameters (anisotropic for W, P, F, O, and C) refined by full-matrix least squares.[24] Hydrogen atoms were placed in idealized fixed positions for the final cycles. An isotropic extinction parameter introduced earlier did not differ significantly from zero and was omitted from the final cycles. A final difference Fourier revealed several peaks (1.2–2.3 e Å^{-3}) in the vicinity of the tungsten atoms but was otherwise featureless.

$W_2(TFA)_4$·3PMe_3. Inside the drybox, a concentrated toluene solution of $W_2(TFA)_4$ was placed in an 8-mm Pyrex tube topped with a Kontes greaseless high-vacuum stopcock. This solution was carefully layered—first with a few millimeters of pure toluene and then with a toluene solution containing 3 equiv of PMe_3. The tube was sealed, removed from the drybox, and left undisturbed for 1 week. Large, dark-green crystals had formed by this time; they were filtered off, washed with a small amount of hexane, and dried in vacuo. A suitable fragment was obtained by cleaving a larger sample inside a nitrogen-filled drybag and transferring to the goniostat. A systematic search of a limited hemisphere of reciprocal space revealed an orthorhombic lattice with systematic absences of $l = 2n + 1$ for $0kl$ and $h + k = 2n + 1$ for $hk0$. Statistical tests, the Patterson synthesis, and successful solution and refinement of the structure led to the assignment of the noncentric space group $Pc2_1n$.[25] Diffraction data were collected at −163 ± 4 °C, and the structure was solved by Patterson and Fourier techniques. ψ scans of several reflections were essentially flat, and due to the irregular shape of the crystal and its small size, no absorption correction was performed. The structure was refined by full-matrix least squares. All atoms, with the exception of the PMe_3 hydrogens, were located and their positional and thermal parameters (anisotropic for W, P, F, O, and C) refined. The atomic coordinates reported are for the proper enantimorph for the crystal chosen, based on residuals for both settings. Hydrogen atoms were placed in idealized staggered positions for the final cycles of the refinement. A secondary extinction parameter introduced in the final cycles did not differ significantly from zero. A final difference Fourier was essentially featureless; the two largest peaks of 1.2 and 1.4 e Å^{-3} were found within 0.5 Å of the two tungstens. Numerous peaks of 0.8–1.2 e Å^{-3} were located in the vicinity of F atoms.

Acknowledgment. The authors are grateful to the National Science Foundation (Grant No. CHE82-06169) for support of this work and the Marshall H. Wrubel Computing Center, Indiana University, for a generous gift of computer time. A.P.S. would also like to thank Professor R. A. Andersen (Cal-Berkeley) for providing us with a preprint of his work on tungsten carboxylate chemistry and for a photocopy of the relevant portions of the Ph.D. thesis of Dr. G. S. Girolomi.

Registry No. 1, 77479-85-7; **2a**, 88888-82-8; **2b**, 88888-83-9; **2c**, 88888-84-0; 3, 88888-85-1; W, 7440-33-7.

Supplementary Material Available: Tables of anisotropic thermal parameters, calculated hydrogen atom positions, and structure factors for **2c** and 3 (18 pages). Ordering information is given on any current masthead page. The complete structural reports (MSC82920, **2c**; MSC82914, 3) are available, in microfiche form only, from the Chemistry Library, Indiana University.

(22) Equivalent positions for $I2/a$ are $^1/_2$, $^1/_2$, $^1/_2$ and 0, 0, 0 ± x, y, z; $^1/_2 - x, y, -z$.

(23) All computations were performed with use of the Indiana University Molecular Structure Center XTEL program library. The XTEL library consists of local programs and code from J. A. Ibers (Northwestern University) and A. C. Larson (Los Alamos Scientific Laboratory).

(24) Neutral-atom scattering factors were from: "International Tables for X-ray Crystallography"; Kynoch Press; Birmingham, England, 1974; Vol. IV. For hydrogen atoms, the values used were given by: Stewart, R. F.; Davidson, E. R.; Simpson, W. T. *J. Chem. Phys.* **1965**, *42*, 3175.

(25) $Pc2_1n$ is a nonstandard setting of $Pna2_1$, with the following equivalent positions: x, y, z; $^1/_2 - x, y, ^1/_2 + z$; $^1/_2 + x, ^1/_2 + y, ^1/_2 - z$; $-x, ^1/_2 + y, -z$.

Contribution from the Department of Chemistry and Laboratory for Molecular Structure and Bonding, Texas A&M University, College Station, Texas 77843

A Metal–Metal-Bonded Dinuclear Phosphine Complex of Niobium(IV) Chloride, $[NbCl_2(PMe_2Ph)_2]_2(\mu\text{-}Cl)_4$

F. ALBERT COTTON* and WIESLAW J. ROTH

Received July 29, 1983

The crystal structure of a compound that was expected to be (and in solution probably is) $NbCl_4(PMe_2Ph)_2$ has revealed a remarkable and unprecedented binuclear structure. The molecule is centrosymmetric and consists of two square-antiprismatic $Nb(PMe_2Ph)_2Cl_6$ units sharing a square Cl_4 face. The outer square faces, which have a trans P_2Cl_2 ligand set, are staggered with respect to the central Cl_4 face. The Nb–Nb distance, 2.838 (1) Å, indicates that a metal–metal single bond is formed. On dissolving in CH_2Cl_2 or THF, this red-brown compound immediately gives a green solution, suggesting that dissociation to $NbCl_4(PMe_2Ph)_2$ molecules accompanies dissolution. The crystals belong to space group $P2_1/n$ with unit cell dimensions of a = 8.545 (2) Å, b = 14.277 (3) Å, c = 19.634 (2) Å, β = 101.33 (1)°, V = 2349 (2) Å^3, and Z = 2. The structure was refined to R = 0.0385 and R_w = 0.0588. Some mean distances are Nb–Cl_b = 2.541 [6] Å, Nb–Cl_t = 2.484 [10] Å, and Nb–P = 2.700 [2] Å.

Introduction

In the course of a lengthy study of the mixed halo–phosphine complexes of tantalum and niobium in oxidation states of IV or less, we have encountered a result sufficiently novel and unexpected that we wish to report it separately. The main body of our work on the stabilities and stereochemistries of $MX_n(PR_3)_x$ species in both the solid state and solution, which is not yet complete, will be reported later.

Because of some unusual features in the behavior of $NbCl_4(PMe_2Ph)_2$ in solution, we decided to determine the crystal structure to see if that information would be helpful. We have found that in the crystal the molecules are dinuclear with an unprecedented type of structure. That structure is described and discussed here.

Experimental Section

Preparation. All manipulations (including later handling of the crystalline product) were carried out in an atmosphere of argon. Niobium(V) chloride and phenyldimethylphosphine were purchased from Aldrich and Strem Chemicals, Inc., respectively, and used as received.

To a 100-mL three-neck flask were added $NbCl_5$ (2.0 g, 7.4 mmol), 40 mL of toluene, and PMe_2Ph (3.5 mL, 24.5 mmol). Sodium

0020-1669/84/1323-0945$01.50/0